Microscopy and Microanalysis (2021), **27**, 923–934
doi:10.1017/S1431927621012010

Microscopy AND Microanalysis

Original Article

Integrated Microscopy and Metabolomics to Test an Innovative Fluid Dynamic System for Skin Explants *In Vitro*

Enrica Cappellozza[1], Serena Zanzoni[2], Manuela Malatesta[1,a] and Laura Calderan[1*a]

[1]Department of Neurosciences, Biomedicine and Movement Sciences, Section of Anatomy and Histology, School of Medicine and Surgery, University of Verona, Verona 37134, Italy and [2]Centro Piattaforme Tecnologiche, Spectroscopy, Diffractometry and Molecular Interaction Study Platform, University of Verona, Verona 37100, Italy

Abstract

The *in vitro* models are receiving growing attention in studies on skin permeation, penetration, and irritancy, especially for the preclinical development of new transcutaneous drugs. However, synthetic membranes or cell cultures are unable to effectively mimic the permeability and absorption features of the cutaneous barrier. The use of explanted skin samples maintained in a fluid dynamic environment would make it possible for an *in vitro* experimentation closer to *in vivo* physiological conditions. To this aim, in the present study, we have modified a bioreactor designed for cell culture to host explanted skin samples. The preservation of the skin was evaluated by combining light, transmission, and scanning electron microscopy, for the histo/cytological characterization, with nuclear magnetic resonance spectroscopy, for the identification in the culture medium of metabolites indicative of the functional state of the explants. Our morphological and metabolomics results demonstrated that fluid dynamic conditions ameliorate significantly the structural and functional preservation of skin explants in comparison with conventional culture conditions. Our *in vitro* system is, therefore, reliable to test novel therapeutic agents intended for transdermal administration in skin samples from biopsies or surgical materials, providing predictive information suitable for focused *in vivo* research and reducing animal experimentation.

Key words: ^{1}H-NMR, bioreactor, correlative microscopy, light microscopy, scanning electron microscopy, skin barrier, transmission electron microscopy

(Received 14 April 2021; accepted 2 June 2021)

Introduction

The skin is a multilayered organ made of epidermis and dermis, each of which characterized by peculiar histological features and unique complementary functions. As an efficient physical, immunological, and sensory barrier, the skin prevents water loss and protects the organism against chemical and physical agents (e.g., UV radiation, chemicals, pathogens); at the same time, skin mediates the relationships between the organism and the external environment (Brazzini et al., 2003). The skin barrier properties mostly rely on the *stratum corneum*, that is, the uppermost epithelial layer composed of differentiated anucleate cells (the corneocytes), which are filled with keratins and embedded in a lipid domain. This highly hydrophobic layer is a so efficient barrier and that it also hampers the uptake of active compounds for local or systemic therapeutic treatments. In fact, the transdermal penetration of chemicals may occur only through the intercellular lipid domains, the keratin bundles in the *stratum corneum*, or the skin appendages (Schaefer & Redelmeier, 1996, 2020; Trommer & Neubert, 2006).

For the development of new transcutaneous drugs, it is, therefore, necessary to use an experimental model able to effectively mimic the permeability and absorption features of the cutaneous barrier. *In vivo* experimentation on laboratory animals remains widely used, going against the trend of the recent decades that would drive toward a Replacement of the animal whenever possible, or at least to a Reduction in its use, and to the Refinement of the methods employed (the so-called 3Rs principle; Russell & Burch, 1959). Due to the recently changed regulatory rules on animal testing, the *in vitro* models are receiving increased attention in the studies on skin permeation, penetration, and irritancy; thus, for the preclinical experimentation of new drugs constructed for cutaneous administration, there is a growing interest for experimental systems able to effectively mimic the permeability and absorption features of the cutaneous barrier.

Currently, the simplest and most used skin model to test pharmaceutical and cosmetic formulations is the Franz diffusion cell system, where the skin is simulated by a synthetic membrane (Ji-Eun et al., 2017; Salamanca et al., 2018). A more complex alternative is represented by the *in vitro* models, the most commonly used being 2D or 3D monocellular cultures or 3D co-cultures. The conventional monolayer cell culture is widely used, but it is a simplistic model, very far from the real complexity of the biological structure (Hansmann et al., 2013; Planz et al., 2016).

[a]These authors contributed equally to this work.

***Author for correspondence:** Laura Calderan, E-mail: laura.calderan@univr.it

Cite this article: **Cappellozza E, Zanzoni S, Malatesta M, Calderan L** (2021) Integrated Microscopy and Metabolomics to Test an Innovative Fluid Dynamic System for Skin Explants *In Vitro*. *Microsc Microanal* **27**, 923–934. doi:10.1017/S1431927621012010

In recent years, research has increasingly been focussed on 3D co-cultures, that is, the culture of different cell types re-creating the morphological and functional complexity of a tissue or an organ (Hansmann et al., 2013). 3D co-cultures are envisaged as an alternative to *in vivo* and *ex vivo* tests due to their high reproducibility and simplicity (Abd et al., 2016) but, again, they are unable to fully reproduce the actual characteristics of the human or animal skin (Dąbrowska et al., 2016). Indeed, these artificial skin equivalents have a different grade of absorption in comparison with the real skin due to their structural and chemical constituents (Godin & Touitou, 2007). Moreover, they are devoid of components, such as the cell junctions, appendages, and vasculature, that greatly influence the penetration of molecules through the skin as well as the immune reaction to damage, pathogens and pathogenic agents (Kendall & Nicolaou, 2013; Mathes et al., 2014; Abaci et al., 2017). Another aspect to be considered in setting up skin 3D co-cultures is the need to ensure the dynamic nutrient intake and removal of waste products along with the entire thickness of the artificial tissue (Brand et al., 2000; Pusch et al., 2011).

The design of bioreactors as fluid dynamic systems allowed a great advance, making it possible to grow cells in an environment with controlled and tuneable parameters, such as medium flow rate, nutrient supply, pH, and temperature (Chen & Hu, 2006; Haycock, 2011; Hansmann et al., 2013). The use of explanted skin samples (from biopsies or surgical materials) maintained in a fluid dynamic environment would make it possible for an *in vitro* experimentation closer to *in vivo* physiological conditions, thus filling the still existing gap between the situation in a living organism and the artificial mimicking models.

To this aim, in the present study, we have modified a bioreactor designed for cell culture to host explanted skin samples; the preservation of the skin was evaluated by combining different microscopy techniques—light microscopy (LM), transmission electron microscopy (TEM), and scanning electron microscopy (SEM), for the histo/cytological characterization, with nuclear magnetic resonance spectroscopy (^{1}H-NMR), for the identification in the culture medium of some metabolites indicative of the functional state of the skin.

Materials and Methods

Skin Explant and Culture

Skin samples were explanted from the abdominal region of six healthy 3-month-old male Wistar rats killed with an overdose of CO_2 according to the regulations of the Italian Ministry of Health (DL March 4, 2014, n. 26, directive implementation 2010/63/UE) and to the European Communities Council (Directive 63/2010/EU of the European Parliament and of the Council) directives. The project was approved by the Italian Ministry of Health (code no. 56DC9. N.703).

Freshly excised skin samples were rapidly washed in physiological solution (NaCl 0.9% w/v) and then in a pre-warmed culture medium at 37°C. The culture medium was composed of DMEM (Dulbecco's Modified Eagle's Medium) supplemented with 4.5 g/L D-glucose, 10% FBS, 2% penicillin–streptomycin, 200 mM L-glutamine and 0.3 μg/mL Amphotericin B (Gibco, Waltham, MA, USA).

Some samples were immediately fixed and processed for LM, TEM, and SEM (see below), and served as controls.

Roundish samples with a diameter of 1.5 cm were cut and mounted in cell culture chambers (LiveBox2, IV-Tech, Massarosa, LU, Italy) suitably modified to hold skin sample in tension as a membrane between the two chambers, with the upper side in contact with air and the lower side in contact with the medium (Fig. 1). The medium was placed into a 16 mL mixing chamber of the bioreactor connected in series to a peristaltic pump (LiveFlow, IV-Tech, Massarosa, LU, Italy)

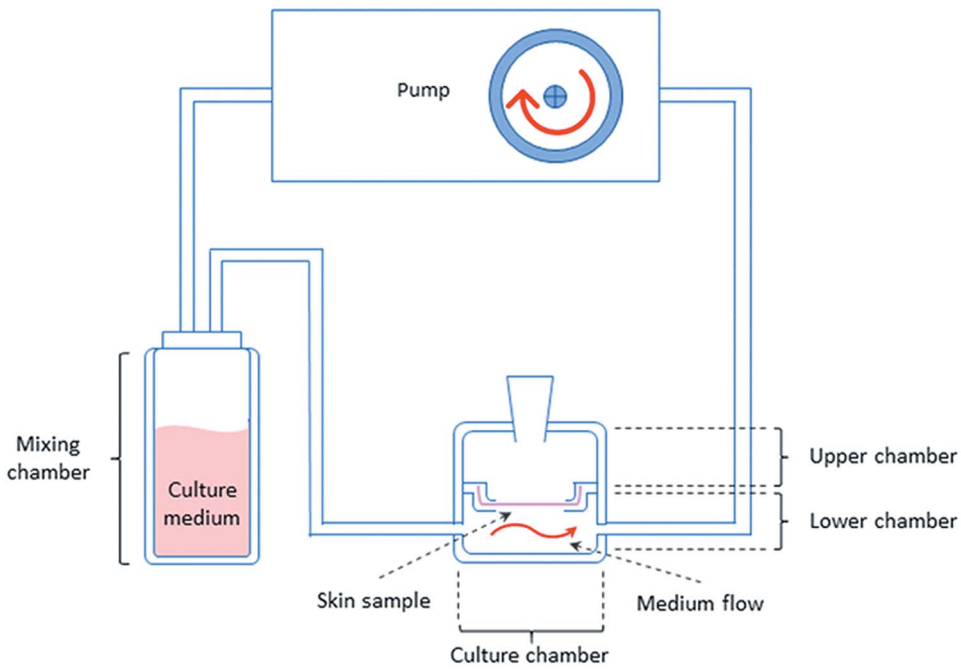

Fig. 1. Scheme of the bioreactor. It consists of a mixing chamber, which provides the reservoir of culture medium, a peristaltic pump, which ensures the medium flow, and modified culture chambers. In the chamber, the skin sample is placed between the lower chamber (where the medium flows) and the upper chamber (with air).

https://doi.org/10.1017/S1431927621012010 Published online by Cambridge University Press

and the lower chambers of four LiveBox2. A flow rate of 500 μL/min was applied. Skin samples were maintained under these fluid dynamic conditions in the incubator, at 37°C in 5% CO_2 humidified atmosphere, for 6, 24, and 48 h. In parallel, skin samples of the same size were maintained for 6, 24, and 48 h at the same experimental settings (culture medium composition, incubation temperature, and humidity), but under conventional conditions, that is, in Petri dishes containing 4 mL of medium (Moll, 2003).

Microscopy Evaluation of Skin Preservation

Skin samples were processed for LM, SEM, and TEM immediately after excision (t0, as control) and at each incubation time (6, 24, and 48 h). In order to prevent catabolites accumulation and improve tissue preservation, the culture medium was changed after 6 and 24 h in both dynamic and conventional conditions.

For histological analysis at bright-field microscopy, skin samples were fixed with 4% paraformaldehyde (v/v) in 0.1 M phosphate buffer overnight at room temperature, dehydrated in ethanol, treated with xylene and finally embedded in paraffin wax. Seven μm thick cross sections (from the outer epidermis surface to the inner hypodermis) were cut, stained with Mayer's hematoxylin and eosin solution (BioOptica, Milan, Italy), mounted in Entellan, and observed with an Olympus BX51 microscope.

For SEM, selected sections used for LM analysis were immersed in 100% xylene for 1 day until the removal of the coverslip and re-immersed in 100% xylene for 1 h to completely remove the mounting medium. After washing with 100% ethanol, samples were gold-sputtered using a MED 010 coater (Balzers) and observed with an XL30 scanning electron microscope (FEI Company, Eindhoven, Netherlands).

For TEM, samples were fixed with 2% (v/v) paraformaldehyde and 2.5% (v/v) glutaraldehyde in 0.1 M phosphate buffer, at 4°C for 3 h, post-fixed with 1% (v/v) OsO_4 and 1.5% (v/v) potassium ferrocyanide for 1.5 h at room temperature, dehydrated with acetone and embedded in Epon-Araldite mixture. Ultra-thin sections (70–90 nm thick) were stained with Reynold's lead citrate and observed with a Philips Morgagni transmission electron microscope (FEI Company Italia Srl), operating at 80 kV and equipped with a Megaview II camera for digital image acquisition.

^{1}H-NMR Analysis of Culture Medium

A metabolomics analysis of the culture medium of skin samples maintained under conventional or dynamic conditions was carried out at increasing incubation times (without medium changes). Aliquots of 1.5 mL of medium were collected per each experimental condition at t0, 6 and 24 h, immediately frozen in liquid nitrogen and placed at −80°C until ^{1}H-NMR analyses. Due to the advanced necrotic state of the samples maintained under conventional conditions (see Section "Results"), no ^{1}H-NMR analyses were performed at 48 h.

Experiments were performed with a Bruker Avance III 600-MHz spectrometer equipped with a TCI cryoprobe operating at 298 K. The samples were defrosted in ice and 500 μL were mixed with 50 μL of D_2O containing TSP, as a reference. The ^{1}H-NMR spectra of the culture media ($n = 3$ for each sample) were obtained by the water-suppressed standard 1D Carr–Purcell–Meiboom–Gill pulse sequence. The free induction decays (FIDs) were recorded by 32 K data points with a spectral width of 7211.54 Hz and 64 scans with a relaxation delay of 4.0 s.

In order to identify the metabolites that changed in different conditions, the NMR spectra were segmented in fixed rectangular buckets of 0.03 ppm width and successively integrated (Bruker Assure NMR software). The spectral region containing the water signal (between 5.10 and 4.7 ppm) was discarded. Each NMR variable was normalized to the total area in order to minimize the small differences due to sample concentration and/or experimental conditions among samples. Metabolites were assigned based on comparisons with the chemical shifts of standard compounds in the Human Metabolome Database (www.hmdb.ca).

Multivariate statistical analysis was performed using MetaboAnalyst 4.0 (https://www.metaboanalyst.ca) to discriminate the high variability and complexity of the spectra and to identify the metabolites that were significant for discriminating between the samples. The principal component analysis (PCA) was initially performed to generate an overview of trends, grouping, and potential outliers in the bucket matrix. Furthermore, to obtain a better separation between groups and identify the significant loadings, the partial least squares-discriminant analysis (PLS-DA) was carried out.

For a biological interpretation of the load carrying the spectral differentiation in the multivariate analysis, we plot the loading for both PC1 and PC2 and assigned the loadings which mainly contributed to the discrimination to their respective metabolites and assessed their values among all tested conditions. Statistical differences of metabolite values between the reference (t0) and the 24 h incubation time and between the two incubation modes at 6 and 24 h were tested by one-way ANOVA followed by Tukey's pairwise test. A value of $p < 0.05$ was considered to be statistically significant.

Results

Microscopy Analyses

At bright-field microscopy, the control samples (t0; Fig. 2a) showed the typical skin architecture composed of two layers above the adipose dermal tissue (the hypodermis). The outer layer, the epidermis is a stratified squamous epithelium composed of keratinocytes. The inner dermis layer in its upper part is made of a dense and compact connective tissue, interfaced with the basal layer of epidermis with which it forms papillae (papillary dermis); in the deeper dermis part, the connective tissue is looser (reticular dermis) and contains adipocytes. The papillary and reticular dermis were merged without clear demarcation. The dermis and the dermal adipose tissue housed the sweat and sebaceous glands (the latter being usually annexed to the hair; Fig. 2a′), hair and hair follicles.

At LM, the skin samples did not show any sign of deterioration in both conventional and dynamic culture systems at all incubation times (Fig. 2): the epithelial layer was intact, the histological continuity between the epidermis and dermis and between the dermis and dermal adipose tissue was preserved, and the annexed structures such as glands and hair follicles were well-maintained. Only after 48 h of incubation in the conventional culture system, a moderate detachment of the glands from the surrounding connective tissue was observed (Fig. 2f′).

On the contrary, correlative SEM evaluations showed a different degree of preservation in the 3D organization of tissues maintained under conventional or dynamic conditions already after 24 h of incubation (Fig. 3). In particular, under conventional

https://doi.org/10.1017/S1431927621012010 Published online by Cambridge University Press

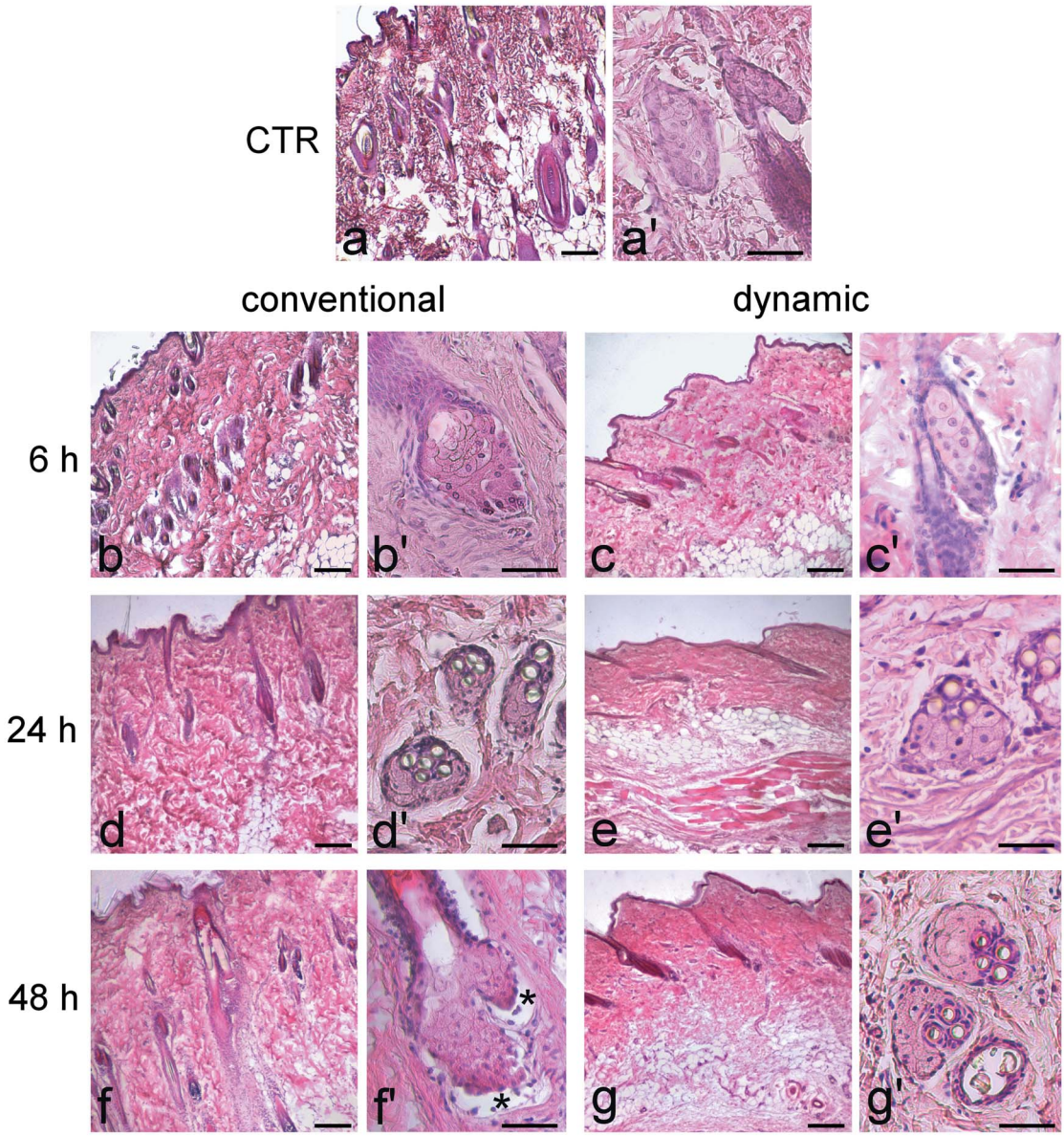

Fig. 2. LM micrographs of skin control samples (CTR) and explants maintained *in vitro* under conventional and dynamic conditions for increasing times. No marked morphological differences are evident, even at higher magnification, apart from a detachment of the sebaceous gland from the surrounding connective tissue in **f**′ (asterisks). Bars: 100 μm (**a**–**g**), 50 μm (**a**′–**g**′).

conditions, the sebaceous glands showed a heavily damaged alveolar structure and connective capsule, and even the fibrillary component of the surrounding connective tissue appeared disorganized (Fig. 3a). Conversely, at the same time point, the sebaceous glands showed a good structural preservation under dynamic conditions (Fig. 3b). SEM observations also revealed the marked alterations of the dermal adipose tissue in the conventional versus dynamic culture system (Figs. 3c, 3d): under conventional conditions, the adipocyte basal lamina was broken (Fig. 3c) and the thin collagen fibers connecting adipocytes were lost, whereas under dynamic conditions, the integrity of adipocytes as well as the surrounding fibrillary network were well preserved (Fig. 3d).

TEM observations of control samples (t0; Fig. 4) revealed the usual ultrastructural features of the different skin cell types. In the epidermis, keratinocytes of the outermost layer (also called corneocytes) appeared as sloughing sheets containing a homogeneous material due to keratin accumulation and loss of cell organelles. The keratinocytes of the underlying layers showed a typical flat shape and were characterized by one nucleus, ovoid mitochondria, well-developed smooth and rough endoplasmic reticulum and Golgi complexes, as well as cytoplasmic structures, such as cytoskeletal bundles and keratohyalin granules typical of specific cell layers. The interdigitated plasma membranes showed many desmosomes. At the edge between the basal epidermis layer and the dermis, a basal lamina was clearly visible. In the dermis, hair follicles showed the hair shaft surrounded by a root sheath composed of flat cells with interdigitated plasma membranes showing desmosomes. Keratin filaments were visible in the inner root sheath cells, while a well-defined basal lamina anchored the outer root sheath cells to the connective tissue. Sebaceous glands were composed of cells rich in lipid droplets

https://doi.org/10.1017/S1431927621012010 Published online by Cambridge University Press

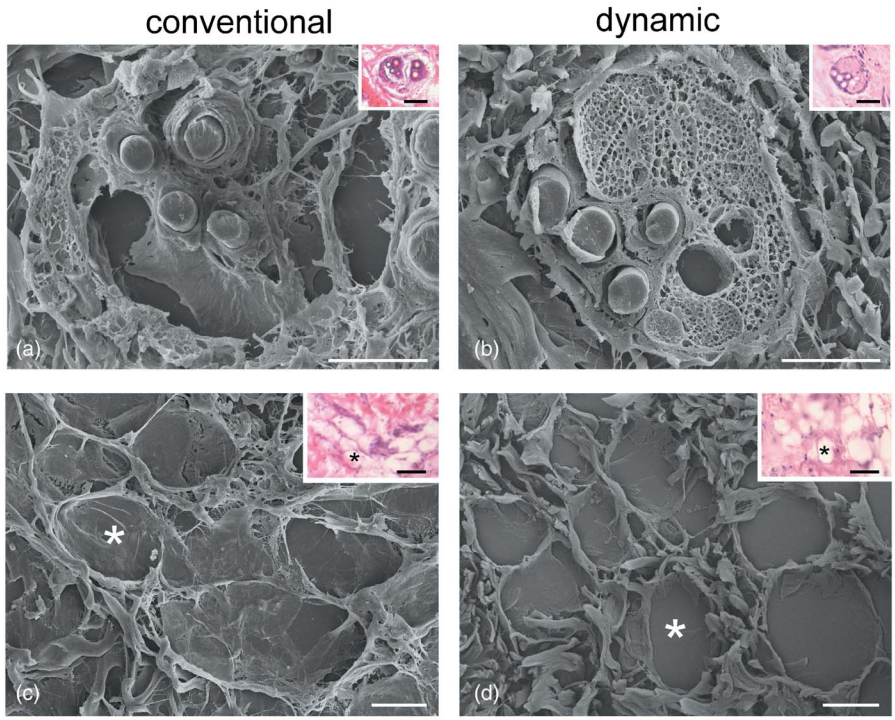

Fig. 3. Correlative LM (insets) and SEM of sebaceous glands (**a,b**) and adipocytes (**c,d**) after 24 h under conventional (**a,c**) and dynamic (**b,d**) conditions. Asterisks indicate the same adipocytes as seen at LM and SEM. Note the good structural preservation in (**b**) and (**d**). Bars: 20 μm. Inset bars: 100 μm.

and mitochondria with tubular cristae. Many fibroblasts and macrophages were distributed in the dermis among irregularly oriented bundles of collagen protein, while many adipocytes occurred in the hypodermis.

After 6 h under conventional conditions, epidermis keratinocytes were quite similar to control samples (t0), but the cells of the hair root sheath, although well preserved, showed enlargements at their boundaries, while sebaceous glands and connective tissue cells (fibroblasts, macrophages, and adipocytes) underwent evident structural alterations (Fig. 5). Under dynamic conditions, the ultrastructural features of all skin cell components were identical with those of control samples.

After 24 h under conventional conditions (Fig. 6), keratinocyte cytoplasm and nucleus appeared as partially emptied, with hardly recognizable organelles, although cell-boundary interdigitations and desmosomes as well as the basal lamina were still preserved; all the other skin cell components were severely damaged. Under dynamic conditions, keratinocytes and cells composing the hair root sheaths were still similar to the control samples (t0), whereas the sebaceous glands and connective cells showed structural alterations.

After 48 h under conventional conditions, both keratinocytes and hair root sheaths were necrotic (Fig. 7), whereas under dynamic conditions, keratinocytes and cells composing the hair root sheaths showed some vacuolization, but the cell organelles, intercellular junctions, and basal lamina were still well recognizable.

^{1}H-NMR Analyses

NMR spectroscopy, together with multivariate statistical analysis, is widely applied for the detection and identification of specific metabolites in culture media that are involved in the tissue metabolism at a specified time and/or under specific environmental conditions (Kosmides et al., 2013; Cisterna et al., 2020). The overlay of the ^{1}H-NMR spectra of all tissue culture media obtained from samples at different times and incubation mode is reported in Figure 8.

Firstly, we used multivariate statistical analysis to examine the presence of an intrinsic variation of the samples incubated in conventional and dynamic conditions and at different times.

The PCA score plot showed that samples were scattered into different regions (Fig. 9a), with the first (PC1, horizontal axis) and second (PC2, vertical axis) principal components contributed to the differentiation, accounting for 44.3 and 12.9.%, of the variation, respectively. The PCA plot revealed a similarity between the control sample and the medium collected from the sample incubated for 6 h under dynamic conditions; the other samples progressively differentiate from the control, with the conventional sample collecting after 24 h being the most distant. Next, to maximize the separation of the groups, PLS-DA was performed. As shown in Figure 9b, PLS-DA showed a good separation pattern with the media samples collected at different times and incubated in different conditions divided into five distinct groups. As expected, the reference sample (culture media at t0) was separated from the media collected after 6 and 24 h, and with the samples collected after incubation in the dynamic mode rather closer to the reference than the media collected from conventional incubation, suggesting a major metabolic variation under the static condition. In order to identify the metabolites that contributed to the cluster separation in the PLS-DA plot, the absolute values of the 2D loading plot obtained for both PC1 and PC2 were plotted, as shown in Figures 9c and 9d.

The main metabolites identified by loading assignments (D-glucose, L-lactic acid, and L-glutamine) and anomalous spectra bins (L-glutamic acid, urocanic acid, and fumaric acid) were

https://doi.org/10.1017/S1431927621012010 Published online by Cambridge University Press

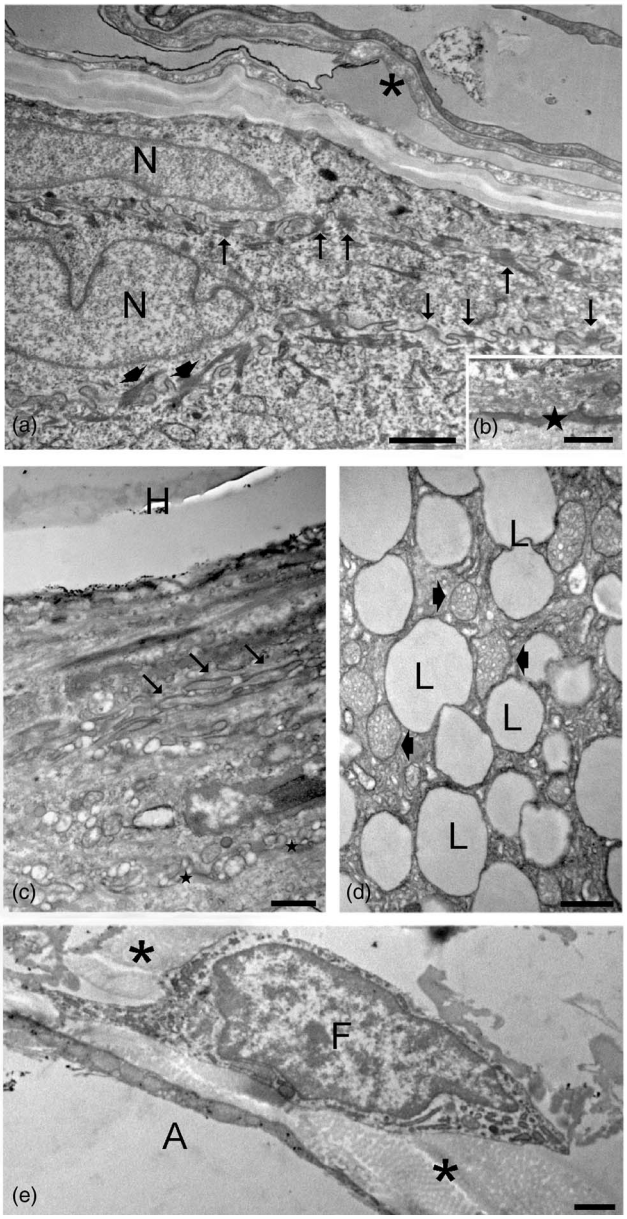

Fig. 4. TEM micrographs of control skin samples. (**a**) Sloughing corneocytes (asterisk) and keratinocytes with elongated nuclei (N), cytoskeletal bundles (arrowheads), and interdigitated plasma membranes with numerous desmosomes (arrows). (**b**) Basal lamina (star) between the basal epidermis layer and the underlying dermis. (**c**) Hair shaft (H) with its root sheath: note the interdigitated plasma membranes (arrows) and the basal lamina (stars) at the borderline with the connective tissue. (**d**) A sebaceous gland with many lipid droplets (L) and mitochondria with tubular cristae (arrowheads). (**e**) A fibroblast (F) and an adipocyte (A) in the dermis; bundles of collagen fibers (asterisks) occur in the extracellular matrix. Bars: 1 μm (**a**,**e**), 500 nm (**c**,**d**), and 200 nm (**b**).

taken into consideration to evaluate the difference in metabolic profiles between the two incubation models (Fig. 10). After 24 h of incubation, an enhanced uptake of glucose and glutamine was observed in the conventional system with respect to the dynamic one, indicative of a higher energy demand. Besides, an increase of lactate release was observed in the same condition. The conventional incubation at 24 h was also characterized by the release of glutamic, fumaric, and urocanic acid in higher amounts than in the dynamic system.

Discussion

In this work, we have tested the suitability of a fluid dynamic system to improve the structural and functional preservation of explanted skin, in order to set up an *in vitro* model close to *in vivo* conditions. To this aim, we have modified a bioreactor originally designed for cell culture that gave excellent results with different cellular models (Vinci et al., 2010, 2011, 2012; Iori et al., 2012; Giusti et al., 2014). The same bioreactor significantly improved the preservation of explanted skeletal muscles in comparison with conventional conditions, thus prolonging the suitability of the organ for *in vitro* tests (Carton et al., 2017).

The modified version of this bioreactor proved to also ameliorate the preservation of skin explants. The morphological evidence demonstrated that all skin explants maintained *in vitro* undergo a progressive deterioration, which affects the histologic components at different times: structural alterations were firstly observed in the sebaceous glands (already after 6 h), then degradation affected connective tissue cells (e.g., fibroblasts and adipocytes) and collagen stroma, and finally, also epithelial cells showed necrotic signs. However, in skin samples maintained under dynamic conditions, this negative drift was delayed so much that, after 48 h in the bioreactor, the cells composing epidermis and hair root sheaths still showed well-preserved organelles and junctions, while skin samples under conventional conditions were completely necrotic.

It is worth noting that these morphological differences were not perceivable at LM but were evident only at electron microscopy, thanks to the higher resolution. In particular, TEM provided evidence of the fine morphology of intracellular organelles and extracellular components, while SEM was especially useful to describe the 3D organization of the fibrillary components of the extracellular matrix, especially the fine fibrils interconnecting adipocytes and anchoring sebaceous glands to the surrounding connective tissue. The correlative analysis at LM and SEM especially highlighted the striking different preservation degree of both glands and fat tissue in samples incubated under dynamic versus conventional conditions.

These findings demonstrate that the simple evaluation of skin sample integrity by means of histological analysis at LM should be considered with caution when performing skin permeability studies, especially when samples are incubated for a long time (Flatena et al., 2015; Planz et al., 2016). In fact, under inadequate incubation conditions, the skin samples may lose their original structural integrity and, consequently, their intrinsic barrier characteristics, thus providing false results on the transcutaneous permeability and biodistribution of active compounds.

The successful preservation of skin samples under fluid dynamic conditions in comparison with conventional conditions is probably related to the increased oxygen/metabolite supply and faster catabolite removal facilitated by the medium flow, while the appropriate levels of temperature, humidity, O_2, and CO_2 are maintained, since the bioreactor used in our study may be placed inside an incubator. Our results are consistent with the study of Yan et al., who described a closed perfusion system to support *ex vivo* skin culture until 12 days *post*-explant, with good preservation of skin layers, cell viability and proliferation (Yan et al., 2019), although the presence of vital and proliferating cells does not guarantee the functional preservation of the physiological skin barrier.

The metabolomic analysis of the culture media supports the morphological observations. It is well known that glucose is the

https://doi.org/10.1017/S1431927621012010 Published online by Cambridge University Press

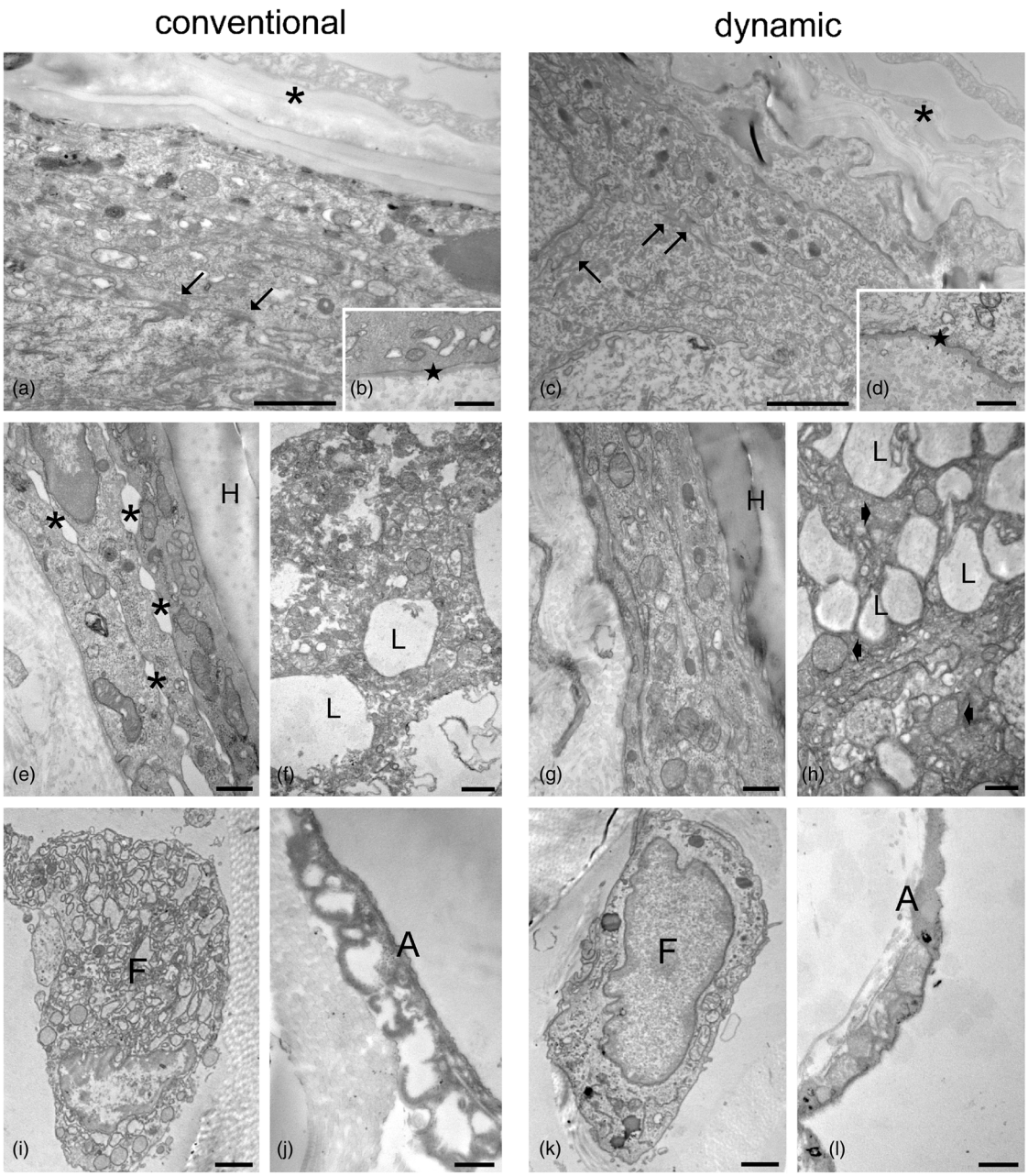

Fig. 5. TEM micrographs of skin samples after 6 h under conventional (**a,b,e,f,i,j**) and dynamic (**c,d,g,h,k,l**) conditions. (**a–d**) Corneocytes (asterisks) and keratinocytes are well preserved in both (**a**) and (**c**). Note the interdigitated plasma membranes with desmosomes (arrows) and the basal lamina (stars in **b**,**d**) between the epidermis and the underlying dermis. Asterisk: corneocytes. The cells of the hair root sheath show enlargements at their boundaries (asterisks) in samples maintained under conventional conditions (**e**), whereas no alteration occurs under dynamic conditions (**g**). H, hair. Sebaceous glands undergo evident damage under conventional (**f**) in comparison with dynamic (**h**) conditions, where lipid droplets and mitochondria (arrowheads) are well preserved. Fibroblasts (F) and adipocytes (A) undergo evident structural alterations under conventional conditions (**i**,**j**), while they are well preserved under dynamic conditions (**k,l**). Bars: 1 μm (**a,c,i,k**), 500 nm (**e–h,j,l**), and 200 nm (**b,d**).

primary source of energy for living organisms and its marked decrease in medium samples from the conventional culture system suggests that this condition leads to a stress state, to which skin cells respond with an increment in energy consumption. At the same time, lactic acid increases, as it normally happens under stress, when the higher glycolytic activity needed to produce energy also increases pyruvate oxidation, from which lactic acid is produced. Generally, it is possible to revert cells to a normal state as long as the mitochondria are intact; conversely, once the mitochondria are damaged, energy failure irreversibly occurs. The accumulation of L-lactic acid in the culture medium under conventional culture conditions is, thus, consistent with the evidence at TEM, where mitochondria appear visibly damaged. Moreover, we can hypothesize that the structural damage of the mitochondria led to the release in the cytosol (and then in the medium) of metabolites such as the fumaric acid, which normally takes part in the Krebs cycle. L-glutamine and L-glutamic acid are key molecules in cell metabolism being fundamental precursors in nucleotide, glucose, amino sugar, and protein biosynthesis, and a primary source of oxidative energy (Tapiero et al., 2002).

https://doi.org/10.1017/S1431927621012010 Published online by Cambridge University Press

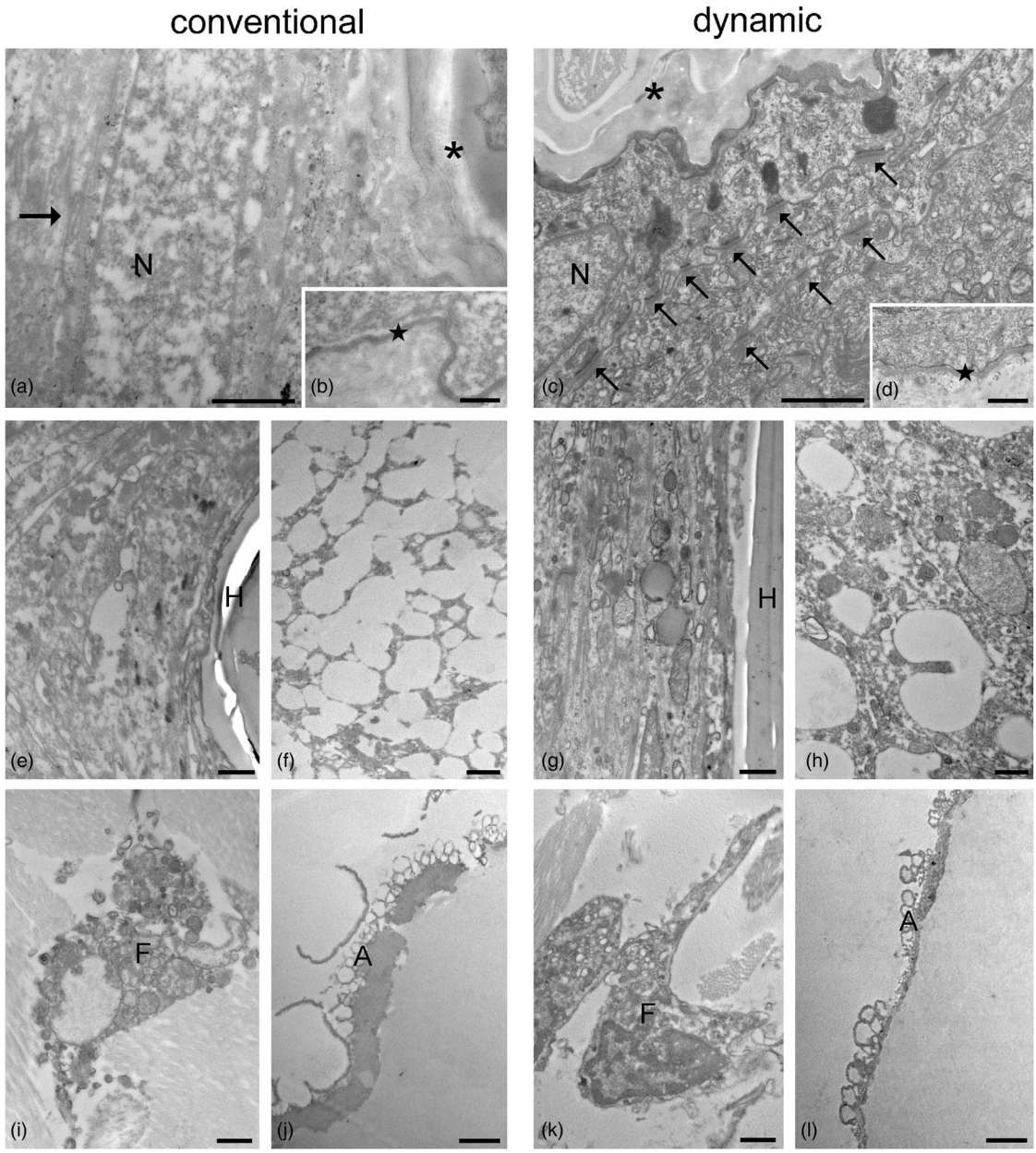

Fig. 6. TEM micrographs of skin samples after 24 h under conventional (**a,b,e,f,i,j**) and dynamic (**c,d,g,h,k,l**) conditions. (**a,b**) Under conventional conditions, keratinocytes appear as partially emptied, although plasma membranes interdigitations (arrows) and the basal lamina (star) are still recognizable. (**c,d**) Under dynamic conditions, no structural alterations are evident in the epidermis: note the numerous well-preserved desmosomes (arrows) and the basal lamina (star). N, nucleus; asterisk, corneocytes. Under conventional conditions (**e**), the cells of the hair root sheath undergo degeneration, whereas no alteration occurs under dynamic conditions (**g**). H, hair. Sebaceous glands undergo evident damage under both conventional (**f**) and dynamic (**h**) conditions. Similarly, fibroblasts (F) and adipocytes (A) show altered features under both conventional (**i,j**) and dynamic (**k,l**) conditions. Bars: 1 μm (**a,c,i,l**), 500 nm (**e–h**), and 200 nm (**b,d**).

Interestingly, the concentrations in the culture media of these two metabolites have an almost complementary trend in all samples, with an increase in glutamic acid corresponding to a decrease in glutamine. This makes us assuming that the increase in glutamic acid concentration is due to the metabolism of glutamine for energy demand, suggesting an alternative pathway for energy request. Moreover, the increase in glutamic acid concentrations leads to a lowering of the medium pH, aggravating the state of cellular stress and suffering. In dynamic culture, this trend appeared to be slowed down compared with the conventional condition, probably thanks to the continuous flow of medium that prevent accumulation of catabolites in close proximity to the tissue while ensuring a continuous supply of metabolites.

Urocanic acid is a typical molecular component of the upper layers of epidermis, where it plays a crucial role in the barrier functions being involved in the absorption of ultraviolet radiation (Krien & Kermici, 2000; Gibbs et al., 2008). The detection of urocanic acid in the culture medium suggests that this molecule diffuses from the stratum corneum to the deeper layers of the skin sample up to the medium because of the degradation of the tissue, as demonstrated by the ultrastructural observations and more relevant for that samples cultured under conventional conditions

https://doi.org/10.1017/S1431927621012010 Published online by Cambridge University Press

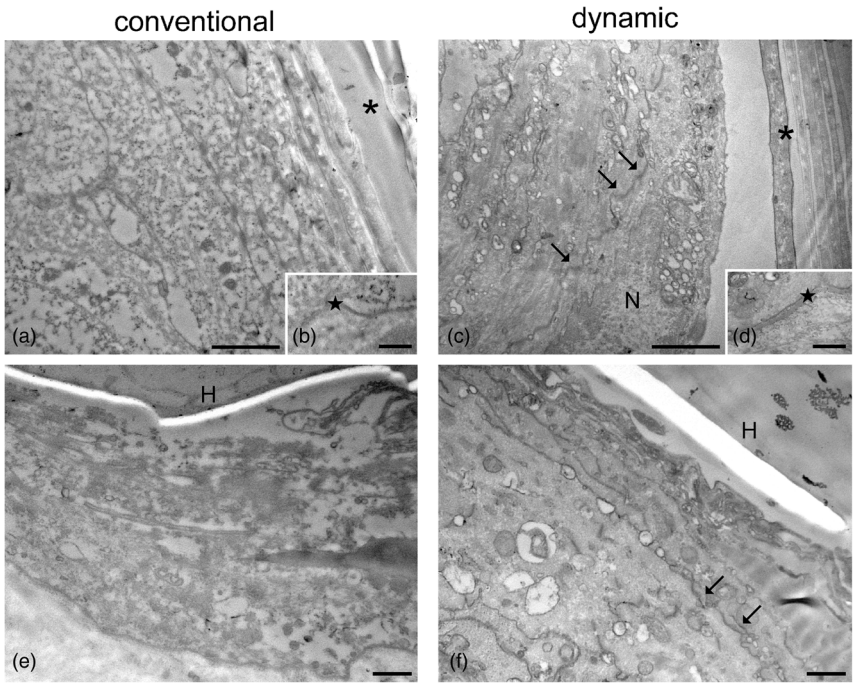

Fig. 7. TEM micrographs of skin samples after 48 h under conventional (**a,b,e**) and dynamic (**c,d,f**) conditions. Under conventional conditions (**a,b**), keratinocytes appear completely necrotic, with a hardly recognizable basal lamina (star), whereas under dynamic conditions, keratinocytes show some vacuolization but plasma membrane interdigitations and desmosomes (arrows) as well as the basal lamina (star) are still preserved. N, nucleus; asterisk, corneocytes. Similarly, under conventional conditions (**e**), the cells of the hair root sheath are necrotic, whereas under dynamic conditions (**g**), although damaged the cells still show well-recognizable cell junctions. H, hair. Bars: 1 μm (**a,c**), 500 nm (**e,f**), and 200 nm (**b,d**).

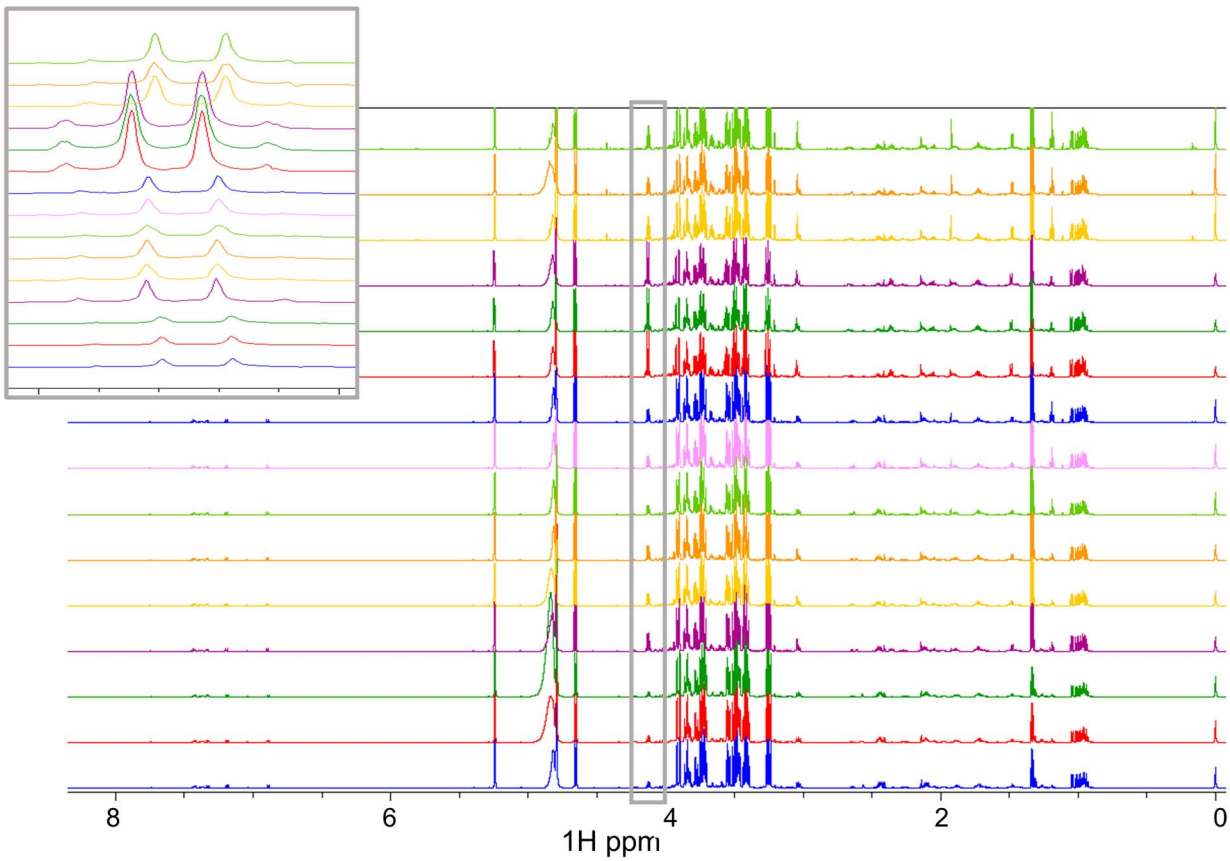

Fig. 8. NMR spectra of all culture media collected after tissue incubation. In the inset, the zoom focused on peaks assigned to lactic acid showing the highest signals in the three samples incubated at 24 h in a conventional mode.

https://doi.org/10.1017/S1431927621012010 Published online by Cambridge University Press

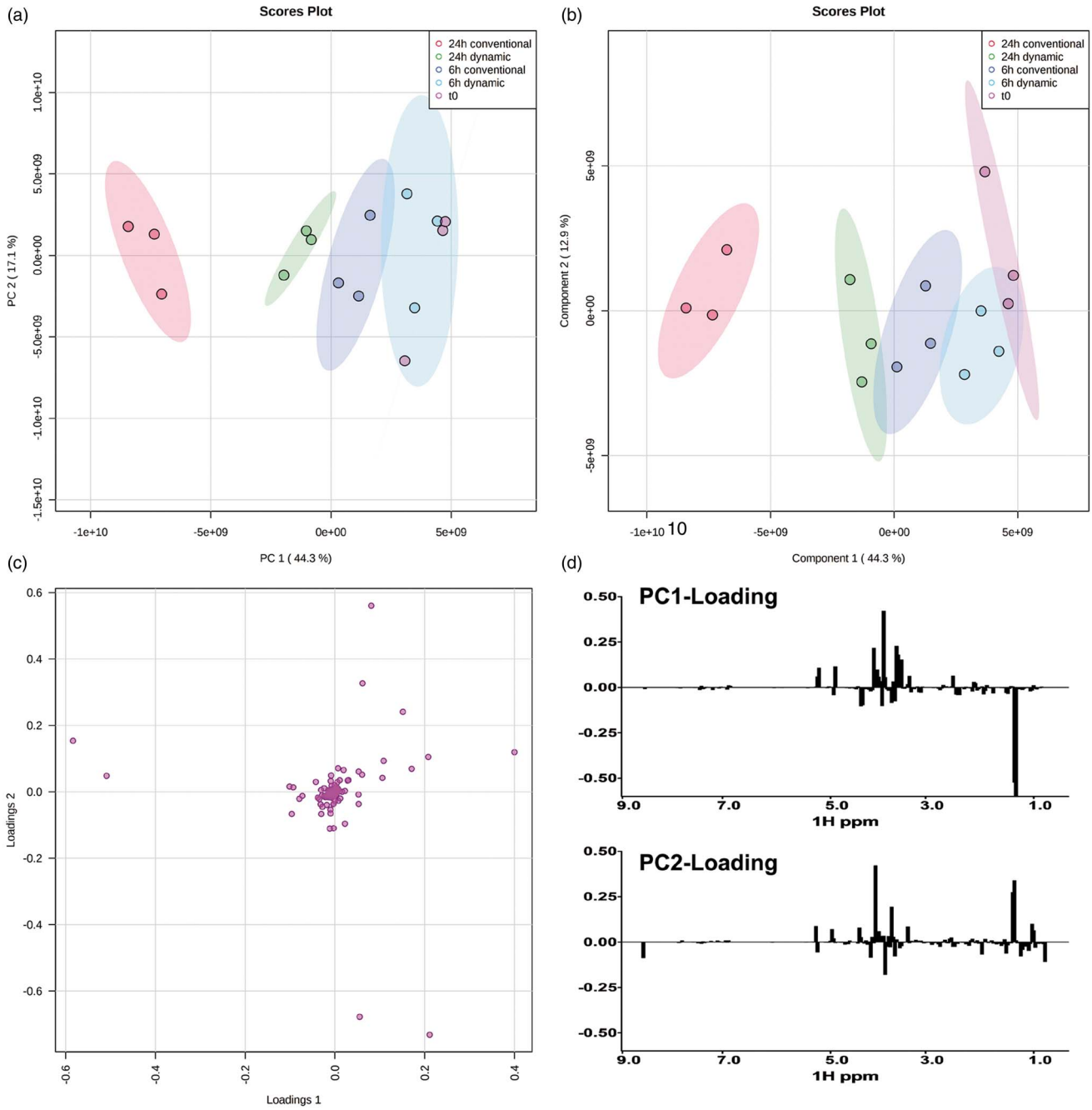

Fig. 9. Multivariate data analysis derived from ^{1}H NMR spectra. (**a**) PCA score plot, (**b**) PLS-DA score plot, (**c**) 2D loading plot generated from PCA, and (**d**) 1D loading plots for PC1 and PC2.

(Solano, 2020). We can, therefore, consider the presence of urocanic acid in the culture medium as a marker of the cellular degeneration occurring in all skin layers, confirming the faster degradation of skin samples maintained in conventional versus dynamic *in vitro* systems.

Conclusion

Taken together, our morphological and metabolomics results highlight the positive contribution of fluid dynamic conditions for both structural and functional preservation of the skin. This implies that the explanted skin maintained in the bioreactor would similarly react to experimental treatments as the skin *in vivo*. Our *in vitro* system is, therefore, reliable to test novel therapeutic agents intended for transdermal administration, thus providing predictive information suitable for focused *in vivo* research. This experimental apparatus can also contribute to the reduction and the refinement of animal experimentation, since it allows performing various tests using skin samples from a single animal. Moreover, we are currently setting up the bioreactor for human skins from biopsy or surgical explants, with the aim of reducing, if not avoiding at all, the preliminary tests on laboratory animals.

https://doi.org/10.1017/S1431927621012010 Published online by Cambridge University Press

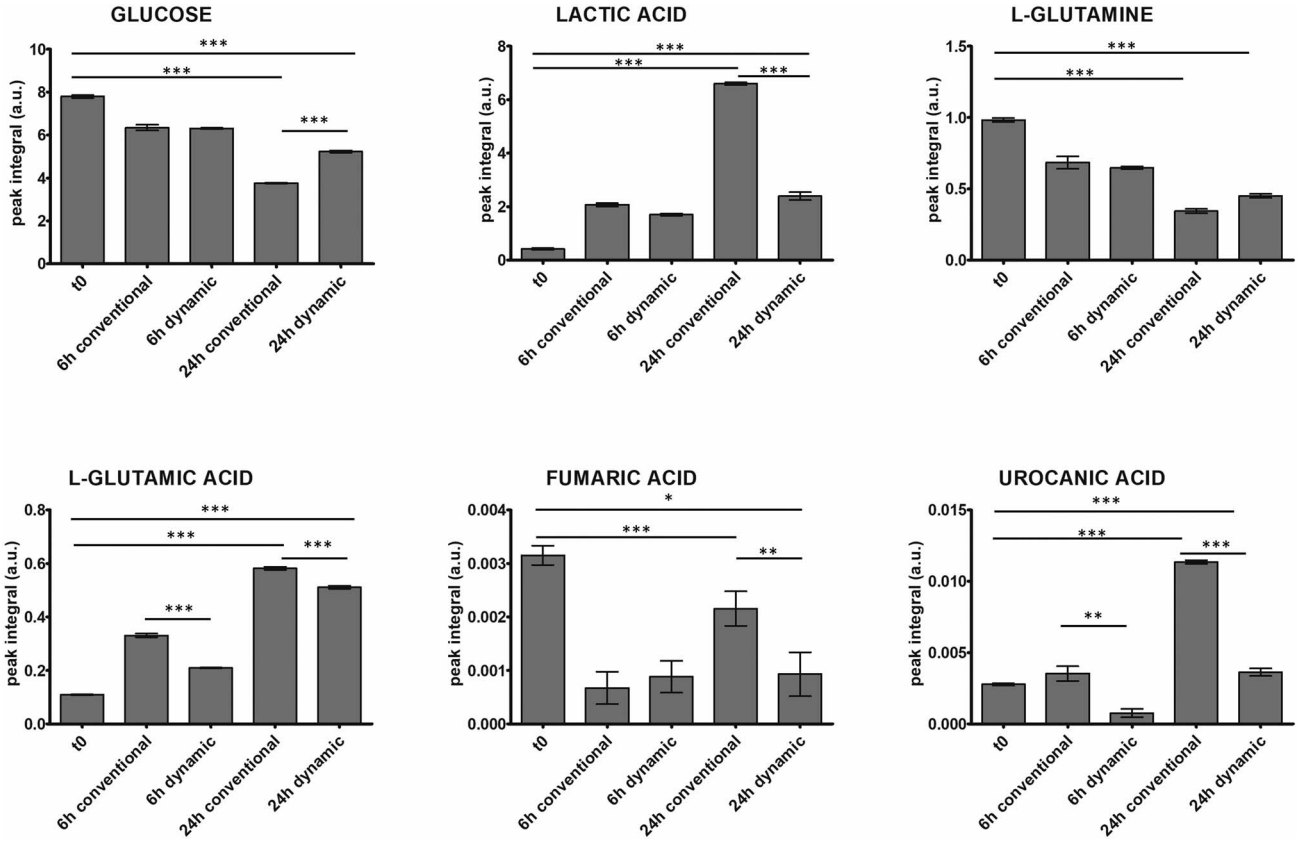

Fig. 10. Bar plots representing differences in the relative concentration of selected metabolites in the media at different incubation mode and times. The arbitrary NMR integral units are reported as mean values ± SE, ($n = 3$). Significant statistical differences of reference (t0) versus the incubation time of 24 h and the differences between the two incubation modes are indicated as ***$p \leq 0.001$, **$p \leq 0.01$.

Acknowledgments. This work was supported by the University of Verona (Joint Projects 2017).

E.C. is a PhD student in receipt of a fellowship from the Doctoral Program "Nanoscience and Advanced Technologies" of the University of Verona.

The authors would like to thank Mr. P. Bernardi for skilful technical assistance in SEM imaging.

Nuclear Magnetic Resonance spectroscopy (^{1}H-NMR) was performed at the *Centro Piattaforme Tecnologiche* of the University of Verona.

References

Abaci HE, Guo Z, Doucet Y, Jacków J & Christiano A (2017). Next generation human skin constructs as advanced tools for drug development. *Exp Biol Med (Maywood)* **242**(17), 1657–1668. doi:10.1177/1535370217712690

Abd E, Yousef SA, Pastore MN, Telaprolu K, Mohammed YH, Namjoshi S, Grice JE & Roberts MS (2016). Skin models for the testing of transdermal drugs. *Clin Pharmacol* **8**, 163–176. doi:10.2147/CPAA.S64788

Brand RM, Hannah TL, Mueller C, Cetin Y & Hamel FG (2000). A novel system to study the impact of epithelial barriers on cellular metabolism. *Ann Biomed Eng* **28**(10), 1210–1217. doi:10.1114/1.1318926

Brazzini B, Ghersetich I, Hercogova J & Lotti T (2003). The neuro-immuno-cutaneous-endocrine network: Relationship between mind and skin. *Dermatol Ther* **16**(2), 123–131. doi:10.1046/j.1529-8019.2003.01621.x

Carton F, Calderan L & Malatesta M (2017). Incubation under fluid dynamic conditions markedly improves the structural preservation in vitro of explanted skeletal muscles. *Eur J Histochem* **61**(4), 2862. doi:10.4081/ejh.2017.2862

Chen HC & Hu YC (2006). Bioreactors for tissue engineering. *Biotechnol Lett* **28**(18), 1415–1423. doi:10.1007/s10529-006-9111-x

Cisterna B, Costanzo M, Nodari A, Galiè M, Zanzoni S, Bernardi P, Covi V, Tabaracci G & Malatesta M (2020). Ozone activates the Nrf2 pathway and improves preservation of explanted adipose tissue in vitro. *Antioxidants (Basel)* **9**(10), 989. doi:10.3390/antiox9100989

Dąbrowska AK, Rotaru GM, Derler S, Spano F, Camenzind M, Annaheim S, Stämpfli R, Schmid M & Rossi RM (2016). Materials used to simulate physical properties of human skin. *Skin Res Technol* **22**(1), 3–14. doi:10.1111/srt.12235

Flatena GE, Palac Z, Engesland A, Filipović-Grčić J, Vanić Ž & Škalko-Basnet N (2015). In vitro skin models as a tool in optimization of drug formulation. *Eur J Pharm Sci* **75**, 10–24. doi:10.1016/j.ejps.2015.02.018

Gibbs NK, Tye J & Norval M (2008). Recent advances in urocanic acid photochemistry, photobiology and photoimmunology. *Photochem Photobiol Sci* **7**(6), 655–667. doi:10.1039/b717398a

Giusti S, Sbrana T, La Marca M, Di Patria V, Martinucci V, Tirella A, Domenici C & Ahluwalia A (2014). A novel dual-flow bioreactor simulates increased fluorescein permeability in epithelial tissue barriers. *Biotechnol J* **9**(9), 1175–1184. doi:10.1002/biot.201400004

Godin B & Touitou E (2007). Transdermal skin delivery: Predictions for humans from in vivo, ex vivo and animal models. *Adv Drug Deliv Rev* **59**(11), 1152–1161. doi:10.1016/j.addr.2007.07.004

Hansmann J, Groeber F, Kahlig A, Kleinhans C & Walles H (2013). Bioreactors in tissue engineering - Principles, applications and commercial constraints. *Biotechnol J* **8**(3), 298–307. doi:10.1002/biot.201200162

Haycock JW (2011). 3D cell culture: A review of current approaches and techniques. *Methods Mol Biol* **695**, 1–15. doi:10.1007/978-1-60761-984-0_1

Iori E, Vinci B, Murphy E, Marescotti MC, Avogaro A & Ahluwalia A (2012). Glucose and fatty acid metabolism in a 3 tissue in-vitro model challenged with normo- and hyperglycaemia. *PLoS ONE* **7**(4), e34704. doi:10.1371/journal.pone.0034704

Ji-Eun S, Sungkyoon K & Bae-Hwan K (2017). In vitro skin absorption tests of three types of parabens using a Franz diffusion cell. *J Expo Sci Environ Epidemiol* **27**, 320–325.

Kendall AC & Nicolaou A (2013). Bioactive lipid mediators in skin inflammation and immunity. *Prog Lipid Res* **52**(1), 141–164. doi:10.1016/j.plipres.2012.10.003

Kosmides AK, Kamisoglu K, Calvano SE, Corbett SA & Androulakis IP (2013). Metabolomic fingerprinting: Challenges and opportunities. *Crit Rev Biomed Eng* **41**(3), 205–221. doi:10.1615/critrevbiomedeng.2013007736

Krien PM & Kermici M (2000). Evidence for the existence of a self-regulated enzymatic process within the human stratum corneum - An unexpected role for urocanic acid. *J Invest Dermatol* **115**(3), 414–420. doi:10.1046/j.1523-1747.2000.00083.x

Mathes SH, Heinz Ruffner H & Graf-Hausner U (2014). The use of skin models in drug development. *Adv Drug Deliv Rev* **69-70**, 81–102. doi:10.1016/j.addr.2013.12.006

Moll I (2003). Human skin organ culture. *Methods Mol Med* **78**, 305–310. doi:10.1385/1-59259-332-1:305

Planz V, Lehr CM & Windbergs M (2016). In vitro models for evaluating safety and efficacy of novel technologies for skin drug delivery. *J Control Release* **242**, 89–104. doi:10.1016/j.jconrel.2016.09.002

Pusch J, Votteler M, Göhler S, Engl J, Hampel M, Walles H & Schenke-Layland K (2011). The physiological performance of a three-dimensional model that mimics the microenvironment of the small intestine. *Biomaterials* **32**(30), 7469–7478. doi:10.1016/j.biomaterials.2011.06.035. Epub 2011 Jul 20.

Russell WMS & Burch RL (1959). *The Principles of Humane Experimental Technique*. London, UK: Methuen & Co.

Salamanca CH, Barrera-Ocampo A, Lasso JC, Camacho N & Yarce CJ (2018). Franz diffusion cell approach for pre-formulation characterisation of Ketoprofen semi-solid dosage forms. *Pharmaceutics* **10**(3), 148.

Schaefer H & Redelmeier TE (1996). *Skin Barrier, Principles of Percutaneous Absorption*. S. Karger AG, P.O. Box, CH-4009 Basel (Switzerland). Printed in Switzerland on acid-free paper by Thür AG Offsetdruck, Pratteln. ISBN: 3-8055-6326-4.

Schaefer H & Redelmeier TE (2020). *Skin penetration. Textbook of Contact Dermatitis*. Springer Nature Switzerland AG. Part of Springer Nature. pp. 209–225.

Solano F (2020). Metabolism and functions of amino acids in the skin. *Adv Exp Med Biol* **1265**, 187–199. doi:10.1007/978-3-030-45328-2_11. PMID: 32761577.

Tapiero H, Mathé G, Couvreur P & Tew KD (2002). II. Glutamine and glutamate. *Biomed Pharmacother* **56**(9), 446–457. doi:10.1016/s0753-3322(02)00285-8

Trommer H & Neubert RH (2006). Overcoming the stratum corneum: The modulation of skin penetration. A review. *Skin Pharmacol Physiol* **19**(2), 106–121. doi:10.1159/000091978

Vinci B, Duret C, Klieber S, Gerbal-Chaloin S, Sa-Cunha A, Laporte S, Suc B, Maurel P, Ahluwalia A & Daujat-Chavanieu M (2011). Modular bioreactor for primary human hepatocyte culture: Medium flow stimulates expression and activity of detoxification genes. *Biotechnol J* **6**(5), 554–564. doi:10.1002/biot.201000326. Epub 2011 Jan 21.

Vinci B, Murphy E, Iori E, Marescotti MC, Avogaro A & Ahluwalia A (2010). Flow-regulated glucose and lipid metabolism in adipose tissue, endothelial cell and hepatocyte cultures in a modular bioreactor. *Biotechnol J* **5**(6), 618–626. doi:10.1002/biot.201000009

Vinci B, Murphy E, Iori E, Meduri F, Fattori S, Marescotti MC, Castagna M, Avogaro A & Ahluwalia A (2012). An in vitro model of glucose and lipid metabolism in a multicompartmental bioreactor. *Biotechnol J* **7**(1), 117–126. doi:10.1002/biot.201100177. Epub 2011 Oct 7.

Yan H, Tang H, Qiu W, Tan R, Zhang W, Yang G & Wu J (2019). A new dynamic culture device suitable for rat skin culture. *Cell Tissue Res* **375**(3), 723–731. doi:10.1007/s00441-018-2945-4. Epub 2018 Nov 3.